

Stiffness-based Understanding and Modeling of Contact Tasks by Human Demonstration

Pavan Sikka

Brenan J. McCarragher

Department of Engineering, F. E. I. T.

The Australian National University

Canberra, ACT 0200, Australia

Email: {pavan,brenan}@faceng.anu.edu.au

Abstract

Programming robots by human demonstration is an effective method for task-level robot programming. Robot programming for contact tasks such as assembly, where both motion and forces need to be controlled, requires an understanding of the interaction with the environment and cannot effectively be accomplished by playing back recorded trajectories. Furthermore, since human demonstration is used to provide the motion and force trajectories, it is also important to include aspects of human movement control in the model of interaction with the environment. In this paper, we present a method of understanding and modeling contact tasks based on end-point stiffness using data obtained by human demonstration. The concept of end-point stiffness has been used both for explaining human movement control and for the control of robots. Experimental results demonstrate the effectiveness of the method in understanding and interpreting the data obtained by human demonstration of contact tasks.

1 Introduction

Programming by human demonstration [4] is an effective method for developing task-level robot programs. In the simplest case, used in many industrial settings, a human operator moves the robot through the trajectory required for the task. The robot then performs the task by playing back the recorded trajectory, either in whole or in part by planning moves through critical points identified on the trajectory by the human operator.

An important class of tasks that is not covered by the above method consists of tasks involving constrained motion requiring contact with the environment [5]. In contrast with robots, human operators are able to specify and perform such tasks easily. Therefore, extending the paradigm of robot programming by human demonstration to contact tasks is an important step towards automating contact tasks such as

robotic assembly. In this paper, we consider the problem of robot programming of contact tasks by human demonstration.

Contact tasks cannot be satisfactorily specified using position alone as the interaction forces need to be controlled as well. For these tasks, programming by human demonstration involves recording both position and force. Since the recorded motion is a result of the interaction between the operator and the environment, the robot needs to control the interaction and hence, the robot cannot perform the task by playing back the recorded position and force trajectories. This leads to the following important requirements for human demonstration-based systems:

1. a model is required to interpret the demonstrated trajectories,
2. the model for interpreting the demonstrated trajectories must also provide the parameters used for robot control, and
3. the model must be based on considerations of human movement control.

Equilibrium-point control is a popular hypothesis for the control of human movement [2, 11]. According to this hypothesis, human muscles act as tunable springs and movement is controlled by specifying the stiffness and the desired equilibrium lengths of the muscles involved in the movement. This hypothesis has also been used in the control of robots for tasks involving contact with the environment and is called stiffness control [13]. It is a simple case of the more general method of impedance control [9]. In impedance control, the robot end-effector is controlled to exhibit the behavior of a desired end-point mechanical impedance.

Thus, stiffness provides a natural concept around which our approach is developed. The data generated

by human demonstration is modeled in terms of stiffness, and the robot can also be controlled using stiffness control.

2 Related Work: Robots and Contact Tasks

Robot programming by human demonstration has been considered by several authors. Delson and West [4] demonstrated a method to compute an optimized position trajectory for the robot for pick-and-place tasks from several human demonstrations of the task. Hirai *et al.* [7, 8] have considered the problem of robot programming by human demonstration for manipulation tasks involving deformable objects. The above approaches deal primarily with acquiring motion trajectories for a robot and do not account for contact with the environment. Recently, Delson and West [5] have extended their approach to include constrained motion during a subtask segment but have not addressed the problem of identifying subtask segments.

Asada and Izumi [1] present an approach to generate robot programs for contact tasks using teaching data. The task is performed by a person guiding a direct-drive robot, and the motion and force data generated is then used to obtain a robot program to perform the task using hybrid force control [12]. Wang *et al.* [15] also present a similar approach to the derivation of compliant motion programs based on human demonstration and hybrid force control. The task is performed by a person using a tele-operated robot. The work presented in these papers uses hybrid force control as the basis for robot programming and does not take human movement skill into account. These approaches also ignore human motion segments containing no movement, a strategy that is not generally valid.

Skill-based performance and learning of tasks by robots is another method by which robots can perform contact tasks. For example, Liu and Asada [10] represent a skill as a map from the process parameter space of the given task to the control actions used to accomplish the task. However, this approach does not consider the basis of human skill and provides little insight into what the task parameters represent.

3 Stiffness from Human Demonstration

The goal of robot programming by human demonstration is to measure the force and the position of an object being manipulated by a human demonstrator and then use this data to generate a program for robot control in terms of a stiffness matrix and a desired trajectory.

We wish to model the relation between the object

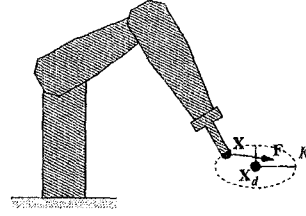


Figure 1: A robot controlled using stiffness

being manipulated and the environment in terms of a generalized spring. Thus, at any instant t , the motion of the object is related to the force acting on the object by the equation:

$$\mathbf{F}(t) = \mathbf{K}(t)[\mathbf{X}_d(t) - \mathbf{X}(t)], \quad (1)$$

where $\mathbf{F}(t)$ refers to the force vector acting on the object, $\mathbf{X}_d(t)$ refers to the desired position of the object, $\mathbf{X}(t)$ refers to the actual position of the object, and $\mathbf{K}(t)$ is the stiffness matrix. The desired position is also called the virtual position. Figure 1 shows the above symbols in the context of a robot arm. In the general case, the force vector is six-dimensional, consisting of the three components of force and the three components of moment. The position vector is also six-dimensional, consisting of the three components of the position of the peg-tip, and the three Euler angles describing the orientation of the peg-tip. \mathbf{K} , the stiffness matrix, is therefore 6×6 .

The goal is to obtain the stiffness matrix from the data generated by human demonstration. Consider m consecutive samples of data obtained over a short interval of time. It is assumed that the desired position and the stiffness matrix do not change over this interval. Then, each pair of $\mathbf{F}(t)$ and $\mathbf{X}(t)$ must satisfy Equation 1.

Since the system must be stable, additional constraints must be imposed on the elements of the stiffness matrix. Thus, the stiffness matrix \mathbf{K} must be symmetric, negative semi-definite.

Physical considerations provide further constraints. All elements in the stiffness matrix must be less than some maximum value since a human operator cannot apply an infinitely large force. Similarly, the maximum deviation from the desired position must also be bounded. Thus, the following constraints are also added to the system:

$$k_{ij} < k_{max},$$

and

$$|\mathbf{X}_d - \mathbf{X}(i)| < \Delta \mathbf{X}_{max}.$$

The stiffness matrix and the desired position can now be obtained by using the standard procedure of

minimizing the square of the error over the time interval in question:

$$\min_{K, \mathbf{X}_d} \int_{t_1}^{t_2} \|\mathbf{F}(t) - K[\mathbf{X}_d - \mathbf{X}(t)]\|^2 dt, \quad (2)$$

subject to the constraints identified above.

4 Sampling Rates and Control of Human Muscles

An important consideration in using the above method is the sampling rate used during the demonstration. This is determined both by the hardware available for measurement and by considerations of how human muscles are controlled during movement.

Human muscles are controlled in a hierarchical manner by the brain [3]. At the lowest level in the hierarchy are the spinal reflexes. These are activated by external disturbances and act in a springlike manner to restore the muscles to their original length. These reflexes occur within 10-20 ms of a disturbance. Long-loop reflexes occur at the next higher level in the hierarchy. These reflexes occur about 40-50 ms after a disturbance and act on groups of muscles, thus allowing some degree of coordinated control over movement. At the highest level in the hierarchy are the long-latency responses which occur about 100 ms after a disturbance and involve structures in the human brain. These are also called voluntary responses.

The delays described above are too large to maintain stability during movement and hence rule out closed-loop feedback control of muscles by the brain. Furthermore, it is known from studies of posture control in humans that when posture is disturbed, muscles respond to stabilize posture about 100 ms after the disturbance. These responses are programmed in nature and activate the joints successively at intervals of 10-20 ms. This suggests that movement control in humans is feed-forward in nature, with several lower level mechanisms available for making corrections to disturbances during the movement.

Since pre-programmed movements can involve changes in muscle stiffness over intervals as short as 10 ms, and since the number of parameters involved is relatively large (10), these considerations impose a very severe constraint on the rate at which human movements need to be sampled to be able to use search procedures mentioned in the previous section.

5 Robot Task Specification from Human Demonstration

An important consideration in interpreting human motion in terms of some model is the number of parameters that need to be determined from the data. Since the sampling rate of the position sensor is of the same

order as the rate at which human muscles are activated in a feed-forward manner, the number of parameters that can be determined from the demonstrated data is small. Thus, we identify a small number of parameters which are used to completely specify the stiffness matrix and the desired trajectory.

The stiffness matrix can be specified geometrically. An arbitrary stiffness matrix expressed in a given reference frame can alternatively be expressed in a related frame in which the off-diagonal elements are 0. Thus, instead of using the demonstrated data to directly obtain the stiffness matrix, we use the data to identify the frame in which the stiffness matrix is diagonal and obtain the diagonal elements. This stiffness matrix can then be expressed in the base reference frame by using a standard geometrical transform. The procedure is described in detail below.

5.1 Interpreting Demonstrated Data using Stiffness

At each instant of the human demonstration, we consider the following 4 situations:

1. Object is stationary in free space,
2. Object is stationary in contact with environment,
3. Object is moving in free space, and
4. Object is moving in contact with environment.

Case 1

In human terms, this situation corresponds to maintaining posture. In studies conducted on human subjects [11, 14], the authors computed the stiffness matrices associated with the human arm in several different postures corresponding to different arm configurations. Since a robot arm is different from a human arm, we experimentally determine the stiffness matrices for the robot arm based on a consideration of the stiffnesses for the human arm obtained by [11, 14] and the kinematic and dynamic parameters of the robot arm. The desired position in this case is taken to be the same as the actual position obtained from the demonstration.

Case 2

This situation corresponds to the demonstrator applying a force on a rigid environment. The only way a force can be exerted using stiffness control is to have a difference between the desired position and the actual position. In humans, a large error between the actual position and the desired position alerts the human and leads to a voluntary response. Thus, to avoid frequent voluntary intervention, the position error must normally be maintained at a small value ΔX_{max} . This value must be determined experimentally from human subjects.

Figure 2 shows the situation corresponding to this case. The frame used to specify a diagonal stiffness

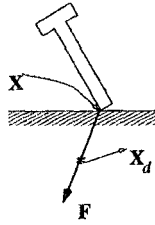


Figure 2: The situation identified in Case 2

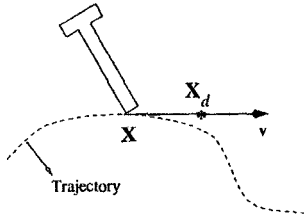


Figure 3: The situation identified in Case 3

matrix is aligned with the direction of the measured force \mathbf{F} . Since there is no other directional information available from the demonstrated data, the other two directions must be chosen arbitrarily. The stiffness along the direction of force is computed from the magnitude of the force divided by the maximum allowed position error ($= \|\mathbf{F}\|/\Delta X_{max}$). The stiffness along the other two directions is specified to be that required to maintain posture, as described for Case 1.

Case 3

This situation corresponds to movement in free space. Recently, Gomi and Kawato [6] studied the variation of human arm stiffness during movements involving multiple joints. Their study indicated that the stiffness tangential to the movement increased significantly during movement as compared to the stiffness when the arm was stationary.

Figure 3 shows the situation corresponding to movement in free space. The desired position is specified tangential to the velocity \mathbf{V} and is calculated using ΔX_{max} ($\mathbf{X}_d = \mathbf{X} + \Delta X_{max} \mathbf{V}$). The frame used to specify the stiffness matrix is aligned with the velocity. The stiffness along this axis is specified to be proportional to the magnitude of the velocity $\|\mathbf{V}\|$. The constant of proportionality depends on the kinematic and dynamic parameters of the robot arm and must be determined experimentally for the robot. Since there is no other directional information available from the demonstrated data, the stiffness along the other two axes must be specified arbitrarily.

Case 4

This situation corresponds to constrained movement and is illustrated in Figure 4. Both velocity and force contribute to the specification of the stiffness matrix and the desired position.

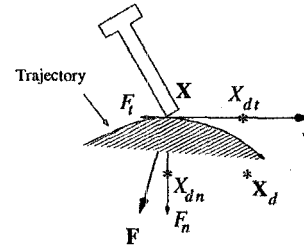


Figure 4: The situation identified in Case 4

The force \mathbf{F} is resolved into tangential and normal components \mathbf{F}_t and \mathbf{F}_n , respectively, with reference to the velocity \mathbf{V} . The first axis of the frame used for specifying the stiffness is aligned with the velocity \mathbf{V} . The second axis of the frame is aligned along \mathbf{F}_n . The third axis is obtained as the cross-product of the first two axes.

The stiffness matrix is obtained using the procedures outlined for Cases 2 and 3. The stiffness along \mathbf{V} is chosen using the procedure outlined for Case 3. However, this stiffness is increased by an amount equal to $\|\mathbf{F}_t\|/\Delta X_{max}$ to account for the additional effort required for the exertion of the tangential force. The stiffness value along \mathbf{F}_n is equal to $\|\mathbf{F}_n\|/\Delta X_{max}$. The stiffness value along the third axis is chosen to maintain posture, as in Case 1.

The desired position is specified in terms of two components \mathbf{X}_{dt} and \mathbf{X}_{dn} , tangential and normal to the velocity \mathbf{V} , respectively. \mathbf{X}_{dt} is obtained using the procedure outlined for Case 3. Similarly, \mathbf{X}_{dn} is obtained using the procedure described for Case 2. Finally, $\mathbf{X}_d = \mathbf{X}_{dt} + \mathbf{X}_{dn}$.

5.2 Further Considerations

This method has an important advantage over the other methods [1, 15] based on hybrid control. In the methods based on hybrid control, the entire demonstration has to be segmented into distinct subtasks, and then each subtask is translated into a control mode (compliance selection matrix) and a set of termination conditions. Since our method is based on stiffness control, it does not require segmentation, and therefore avoids the need for switching control laws and for computing termination conditions. Abrupt changes in stiffness can easily be removed by a smoothing operation applied to the sequence of stiffness values obtained from the demonstration.

An important consideration is the "expertise" of the operator demonstrating the task. Humans quickly learn to perform tasks with repeated practice. The demonstrated data reflects the level of skill attained by a person as they improve their performance on a particular task. For robot programming by human demonstration, it is important that the demonstra-

tions be obtained by people who are considered experts at the task. For example, the situation described in Case 2 can arise either because the person is hesitating or exploring or because the person is deliberately applying a required force. In earlier approaches [1, 15], such segments in the demonstration data are ignored which is generally not correct.

6 Human Demonstration: Experimental Setup and an Example

The primary requirement for human demonstration is the ability to measure the object position and the interaction force as the object is moved by a human demonstrator. The object position is measured using a position tracker connected to the object. The tracker is based on electro-magnetic principles and is manufactured by the Polhemus Corporation. The system provides the position and orientation of a frame attached to the tracker, $\{P\}$, with respect to a frame attached to the base unit, $\{B\}$. The interaction force is measured using a six-axes force sensor manufactured by the JR3 Corporation. This sensor provides the three components of force and the three components of moment with reference to a frame attached to the sensor body, $\{F\}$. The limiting sampling period of the overall setup is about 8.25 ms which is as fast as the position sensor can measure position.

The experimental setup is illustrated in Figure 5. The task consists of moving a long, rectangular peg through a three-dimensional maze. The maze is constructed by cutting a groove in the $x-y$ plane. This groove defines the path to be followed in moving through the maze. The three-dimensional aspect is introduced by the introduction of steps within the groove that impede the motion of the peg in the groove. The path to be followed by the peg-tip is shown in Figure 6(a). The force sensor is mounted under the base of the maze and the position tracker is attached to the base of the peg.

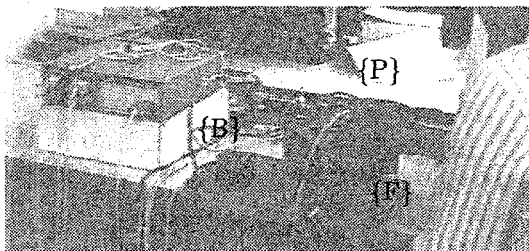


Figure 5: The experimental setup used for human demonstration.

This arrangement provides a significant advantage

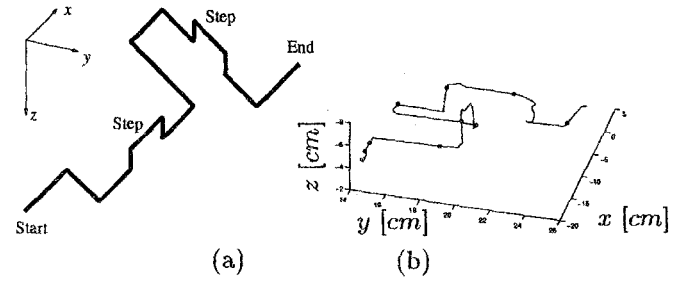


Figure 6: The 3-dimensional path to be followed by the peg-tip. (a) Path geometry. (b) Actual path followed during a demonstration. The circles indicate progress along the path in 1 s intervals.

over the methods used in other studies [1, 15] to collect data from human demonstration. Asada and Izumi [1] used a direct-drive robot arm driven directly by the human demonstrator, whereas Wang *et al.* [15] used a tele-operated robot for task demonstration. Our approach allows the human demonstrator to work more naturally and thus the generated data closely represents human motion.

Since we are interested in the movement of the tip of the peg, we attach a frame $\{T\}$ to the tip. The data obtained from the sensors can be transformed using these frames to describe the motion of the peg-tip with respect to the base frame of the position sensor. Thus, we obtain the sequence of position and force vectors, $\{X(i)\}$ and $\{F(i)\}$, respectively, from a human demonstration of the movement of the peg through the maze.

The shape of the maze is illustrated by the movement of the peg-tip during a demonstration, as shown in Figure 6(b). The force acting at the tip of the peg is shown in Figure 7.

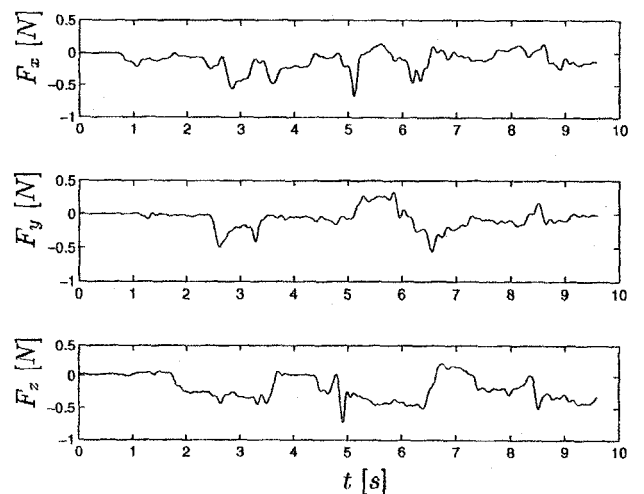


Figure 7: The x -, y -, and z - components of force plotted as a function of time.

The position data was numerically differentiated to

obtain the velocity. The velocity and force are represented using spherical coordinates to show the magnitudes and directions. Thus, Figure 8 shows the velocity in spherical coordinates (with respect to the base frame of the position sensor) while Figure 9 shows the demonstrated force expressed in spherical coordinates. Figure 10 shows each point classified into one of the four situations discussed above. The blank portions within the force and velocity plots correspond to situations where the force or velocity are 0 and so the vector directions are not defined. This figure shows that most of the sampled data from the demonstration is identified into Cases 2 and 4 corresponding to an applied force only and to constrained motion involving both movement and force, respectively. However, the oscillations between these two states, evident in parts of the demonstrated trajectory, indicate the inconsistent nature of human movement and the need for a method to “smooth out” the demonstrated data.

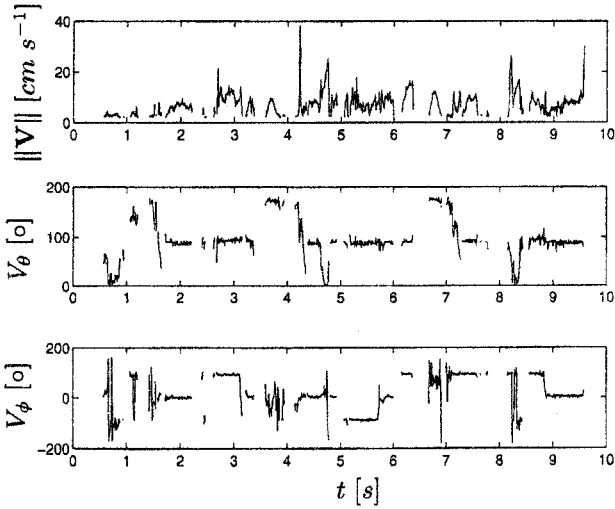


Figure 8: *The spherical components of demonstrated velocity.*

The procedure outlined in Section 4 is used to obtain the end-point stiffness and the desired position for each sample point in the demonstrated data. Figure 11 shows the acquired stiffness values along the three main axes, while Figure 12 shows the desired trajectory. The actual trajectory is also shown for comparison.

A comparison of the desired trajectory and the actual trajectory shows that the trajectory errors increase whenever there is movement while the desired trajectory is almost the same as the actual trajectory for segments involving little or no motion. The stiffness values also show an increase whenever there is motion along the corresponding axis. This indicates that the procedure uses a combination of stiffness and position error to achieve motion, which is how stiffness control works. A second feature is that the x and y

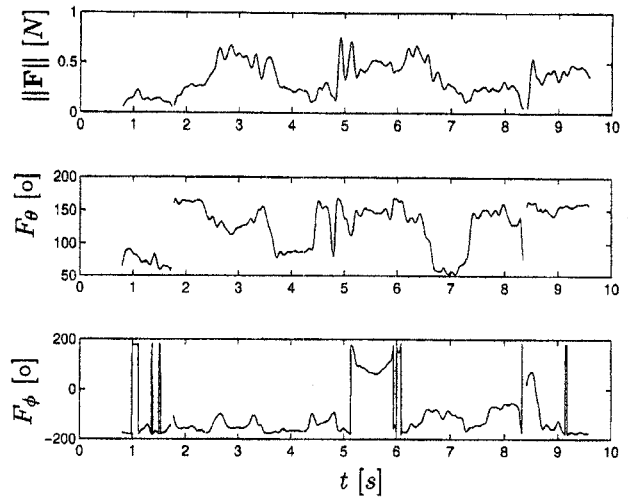


Figure 9: *The spherical components of demonstrated force.*

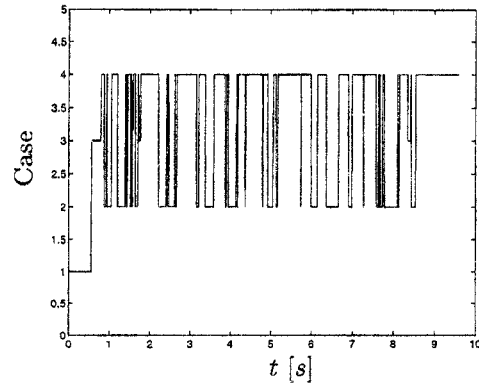


Figure 10: *The demonstrated data classified into one of the four cases identified before.*

components of the desired trajectory are smooth compared to the z component. This is due to the task requirement of force control along z and movement along x and y and indicates that force control is more difficult compared to just movement.

The above discussion shows that the procedure described in Section 4 can provide a satisfactory interpretation of the demonstrated data in terms of stiffness. However, the results also indicate a need for further interpretation before the desired trajectory and the stiffness obtained by this procedure can be used for robot control. We are currently implementing stiffness control on a robot arm to experimentally demonstrate the effectiveness of the methodology presented in this paper for robot programming of contact tasks by human demonstration.

7 Conclusion

We considered the problem of interpreting and modeling of contact tasks by human demonstration. The

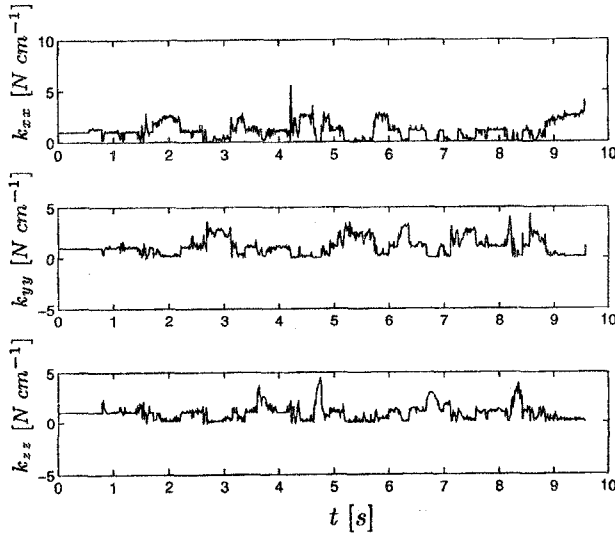


Figure 11: The stiffness values obtained from the demonstrated data.

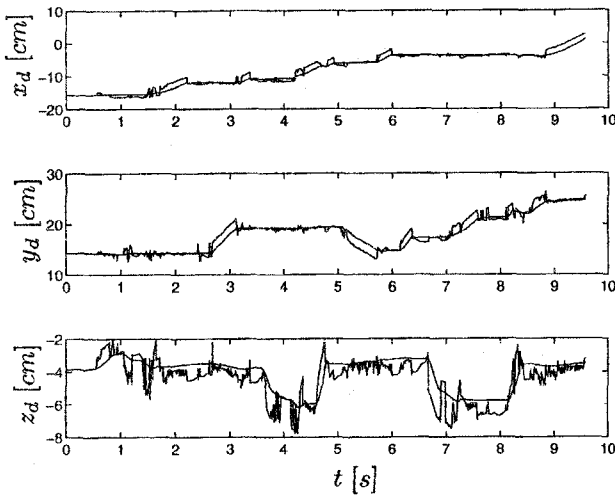


Figure 12: The desired trajectory and the demonstrated trajectory.

problem is significantly more complicated compared to robot programming of motion by human demonstration because of a need for a model of contact that can be used for both robot control and for modeling the data obtained by human demonstration. We considered stiffness control as the model for contact tasks and interpreted the result of human demonstration in terms of stiffness. The results show that the procedure described in this paper is an effective method for interpreting demonstrated data in terms of end-point stiffness. We are currently working to extend this approach to robot programming of contact tasks by human demonstration using stiffness control.

References

- [1] H. Asada and H. Izumi. Automatic program generation from teaching data for the hybrid control of robots. *IEEE Transactions on Robotics and Automation*, 5(2):166–173, Apr. 1989.
- [2] E. Bizzi, N. Hogan, F. A. Mussa-Ivaldi, and S. Giszter. Does the nervous system use equilibrium-point control to guide single and multiple joint movements? *Behavioral and Brain Sciences*, 15:603–613, 1992.
- [3] V. B. Brooks. *The Neural Basis of Motor Control*. Oxford University Press, 1986.
- [4] N. Delson and H. West. Robot programming by human demonstration: The use of human inconsistency in improving 3d robot trajectories. In *The IEEE/RSJ Conference on Intelligent Robots and Systems*, pages 1248–1255, 1994.
- [5] N. Delson and H. West. Robot programming by human demonstration: Adaptation and inconsistency in constrained motion. In *IEEE International Conference on Robotics and Automation*, 1996.
- [6] H. Gomi and M. Kawato. Equilibrium-point control hypothesis examined by measured arm stiffness during multijoint movement. *Science*, 272:117–120, 1996.
- [7] S. Hirai, H. Noguchi, and K. Iwata. Transplantation of human skillful motion to manipulators in insertion of deformable tubes. In *IEEE International Conference on Robotics and Automation*, pages 1900–1905, 1995.
- [8] S. Hirai, H. Noguchi, and K. Iwata. Human-demonstration based approach to the recognition of process state transitions in insertion of deformable tubes. In *IEEE International Conference on Robotics and Automation*, 1996.
- [9] N. Hogan. Impedance control: An approach to manipulation, parts i – iii. *The ASME Journal of Dynamic systems, Measurement and Control*, 107:1–24, 1985.
- [10] S. Liu and H. Asada. Transfer of human skills to robots: Learning from human demonstrations for building an adaptive control system. In *American Control Conference*, pages 2607–2612, 1992.
- [11] F. A. Mussa-Ivaldi, N. Hogan, and E. Bizzi. Neural, mechanical, and geometric factors subserving arm posture in humans. *The Journal of Neuroscience*, 5(10):2732–2743, Oct. 1985.
- [12] M. H. Raibert and J. J. Craig. Hybrid position/force control of manipulators. *The ASME Journal of Dynamic systems, Measurement and Control*, 102, 1981.
- [13] J. K. Salisbury. Active stiffness control of a manipulator in cartesian coordinates. In *IEEE Conference on Decision and Control*, pages 95–100, 1980.
- [14] T. Tsuji, P. G. Morasso, K. Goto, and K. Ito. Human hand impedance characteristics during maintained posture. *Biological Cybernetics*, 72(6):475–485, 1995.
- [15] Q. Wang, J. De Schutter, W. Witvrouw, and S. Graves. Derivation of compliant motion programs based on human demonstration. In *IEEE International Conference on Robotics and Automation*, pages 2616–2621, Apr. 1996.